TRENDS IN SCIENCES 2026; 23(7): 12698
https://doi.org/10.48048/tis.2026.12698 RESEARCH ARTICLE

Hemodynamic and Molecular Effects of F-43 in Experimental Hypertension

Ikbolkhon Abdurazakova[1,*], Anvar Zaynabiddinov[2], Izzatullo Abdullaev[3], Ulugbek Gayibov[3,4], Ziyodullo Ziyoyiddinov[4], Lazizbek Makhmudov[3] and Sherzod Zhurakulov[5]

[1]*Fergana Institute of Public Health, Fergana, Uzbekistan*
[2]*Human Physiology and Safety, Andijan State University, Andijan, Uzbekistan*
[3]*Plant Cytoprotectors, Institute of Bioorganic Chemistry named after A. Sadykov, Tashkent, Uzbekistan*
[4]*Natural Sciences, National University of Uzbeksitan, Tashkent, Uzbekistan*
[5]*Institute of the Chemistry of Plant Substances, Uzbekistan Academy of Sciences, Tashkent, Uzbekistan*

([*]Corresponding author's e-mail: abdurazakovaiqbolxon@gmail.com)

Received: 18 November 2025, Revised: 9 December 2025, Accepted: 16 December 2025, Published: 25 February 2026

Abstract

Hypertension is closely associated with impaired calcium regulation in vascular smooth muscle, leading to sustained vasoconstriction and elevated peripheral resistance. This study investigates the hemodynamic activity of a newly synthesized tetrahydroisoquinoline derivative, F-43 (1-(4′-methoxyphenyl)-6,7-dimethoxy-1,2,3,4-tetrahydroisoquinoline), produced via a modified Pictet–Spengler reaction. Hemodynamic responses were assessed in conscious rats (n = 3 per group) using tail-cuff plethysmography at doses of 25 and 50 mg/kg, including evaluation in an adrenaline-induced hypertension model. F-43 produced a mild transient rise in arterial pressure followed by a statistically significant normalization phase (p-*value* < 0.05), demonstrating a modulatory rather than purely hypotensive profile. In the adrenaline-induced model, F-43 (50 mg/kg) significantly reduced systolic and diastolic elevations within three hours (p-*value* < 0.01), restoring values close to baseline. No acute adverse effects or behavioral abnormalities were observed at the tested doses. To explore potential mechanisms, simplified molecular docking screening was performed, showing favorable binding energies (–6.4 to –8.7 kcal/mol) toward key calcium-handling proteins, suggesting possible interaction with Cav1.2, SERCA, RyR2, and NCX. These *in silico* findings support the hypothesis that F-43 may influence intracellular Ca^{2+} flux, consistent with the observed hemodynamic effects. In conclusion, F-43 demonstrates a unique vascular tone–stabilizing effect, statistical efficacy in an acute hypertension model, and an acceptable preliminary safety profile. The compound represents a promising novel lead molecule for further development of calcium-modulating antihypertensive agents.

Keywords: Adrenaline-induced hypertension, Antihypertensive activity, Aalcium channel modulation, F-43 compound, Molecular docking

Introduction

Hypertension remains one of the most prevalent cardiovascular disorders worldwide, contributing substantially to morbidity and mortality through complications such as ischemic heart disease, stroke, and renal dysfunction [1]. Although several antihypertensive drug classes exist, including calcium channel blockers, β-adrenergic antagonists, and ACE inhibitors, a significant proportion of patients still fail to achieve adequate blood pressure control or experience undesirable side effects. These shortcomings emphasize the need for novel compounds with improved mechanistic specificity and safety profiles. Vascular smooth muscle contraction is primarily governed by intracellular Ca^{2+} dynamics, which depend on the coordinated activity of L-type Ca^{2+} channels (Cav1.2), ryanodine receptors (RyR2), SERCA pumps, and the Na^{+}/Ca^{2+} exchanger (NCX). Dysregulation of these

systems promotes sustained vasoconstriction and elevated peripheral resistance—central features of hypertension [2,3]. However, many current calcium-modulating agents target only one component of this regulatory network, which may limit their efficacy and contribute to tolerance development. Tetrahydroisoquinoline derivatives represent a promising structural class with reported antioxidant, neuroprotective, and calcium-modulatory activities [4,5]. Based on this scaffold, we developed a novel derivative—1-(4′-methoxyphenyl)-6,7-dimethoxy-1,2,3,4-tetrahydroisoquinoline (F-43)—designed to achieve balanced modulation of multiple calcium-handling proteins. We hypothesized that F-43 would exert stabilizing effects on vascular tone by influencing intracellular Ca^{2+} flux through interactions with Cav1.2, SERCA, RyR2, and NCX. This study therefore aimed to evaluate the hemodynamic effects of F-43 in normotensive rats and an adrenaline-induced hypertension model, and to complement these findings with molecular docking simulations to characterize its interactions with key calcium-regulatory proteins [6,7]. By integrating *in vivo* and *in silico* evidence, we sought to define the therapeutic potential of F-43 as a mechanistically novel calcium-modulating antihypertensive agent.

Materials and methods

Synthesis of F-43 compound

The compound F-43 (1-(4′-methoxyphenyl)-6,7-dimethoxy-1,2,3,4-tetrahydroisoquinoline) was synthesized following a modified Pictet–Spengler condensation method described. (Molecules, 2023, 28, 477). Briefly, 3,4- dimethoxyphenylethylamine (0.015 mol) was reacted with an equimolar amount of 4-methoxybenzaldehyde in 10 - 20 mL of trifluoroacetic acid under reflux for 4 - 6 h. The progress of the reaction was monitored by thin-layer chromatography (TLC). After completion, the reaction mixture was cooled and neutralized to pH 9 - 10 using 10% NaOH, followed by exhaustive extraction with chloroform (4×50 mL). The combined organic layers were dried over anhydrous Na_2SO_4 and concentrated under reduced pressure. The crude product was recrystallized from acetone and converted into its hydrochloride salt, which was purified by recrystallization from ethanol [8]. The final free amine, designated as F-43, was obtained after basification to pH 8 - 9, drying, and vacuum evaporation (**Scheme 1**).

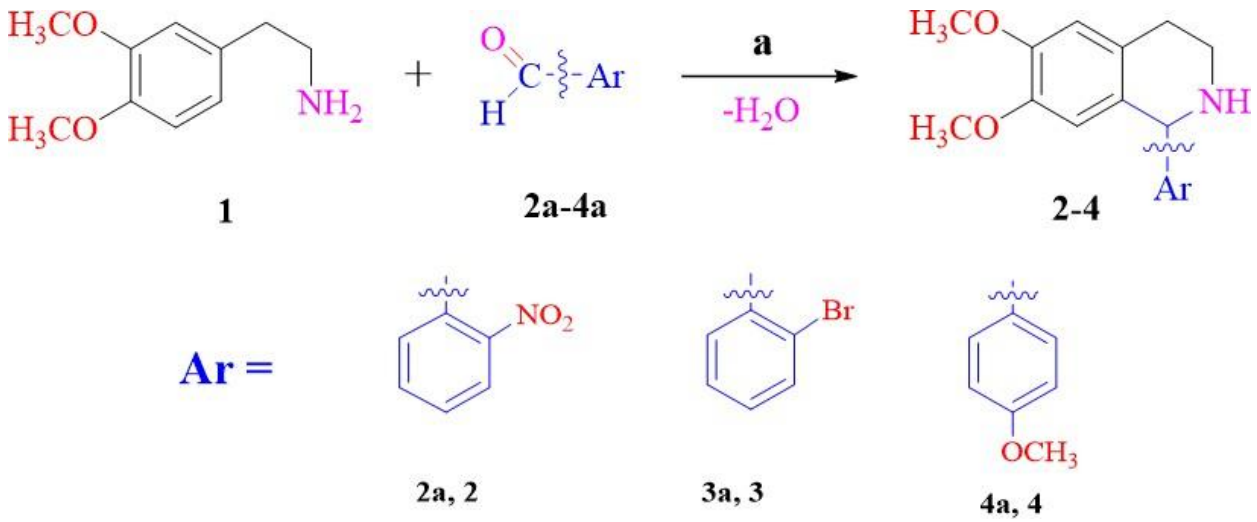

Scheme 1 Synthesis of 1-aryl-6,7-dimethoxy-1,2,3,4-tetrahydroisoquinoline derivatives 2-4.

Animal ethics

All experimental and preoperative procedures were reviewed and approved by the Institutional Animal Care and Use Committee. The animals were maintained in the institutional vivarium under standardized environmental conditions: Temperature of 22 ± 2 °C, relative humidity of 55% - 65%, and ad libitum access to standard laboratory chow and water. All procedures

involving animals were conducted in accordance with the European Directive 2010/63/EU on the protection of animals used for scientific purposes. Ethical approval for the study was obtained from the Animal Ethics Committee of the Institute of Bioorganic Chemistry, Academy of Sciences of the Republic of Uzbekistan (Protocol No. 133/1a/h).

Blood pressure measurements

Blood pressure was recorded using the tail-cuff plethysmography method with the Sistola system (Neurobotics, Russia) after a three-day acclimatization period to minimize stress-related variability (**Figure 3**). Each measurement session included three consecutive readings per animal to ensure reproducibility and accuracy of the data. All experimental assessments were carried out at the "BFM Pharmacology and Screening Laboratory" and the "Plant Cytoprotectors Laboratory" of the A. Sodikov Institute of Bioorganic Chemistry [9,10].

Molecular docking: Software and databases

All computational tools used in this study were freely available for academic and educational purposes. Three- dimensional structural data of calcium-regulatory macromolecules were retrieved from the Protein Data Bank (PDB), an internationally recognized archive of biomolecular structures. The target proteins selected for molecular docking included the L-type calcium channel Cav1.2 (PDB ID: 6JP5), sodium–calcium exchanger NCX1 (PDB ID: 8SGI), ryanodine receptor type 2 RyR2 (PDB ID: 5C33), and sarcoplasmic/endoplasmic reticulum Ca^{2+}-ATPase (SERCA, PDB ID: 6RB2). Ligand structures, including reference compounds and the flavonoids of interest, were initially drawn and constructed using ChemDraw (PerkinElmer, USA). The generated 2D structures were then converted to 3D conformations and geometrically optimized in Avogadro software employing the MMFF94 force field to minimize potential energy and ensure stable configurations. For validation and cross-referencing, structural information and physicochemical data were retrieved from the PubChem database, which provides detailed annotations on molecular properties, pharmacological activity, biological targets, and metabolic pathways. Each PubChem entry integrates more than 80 curated data fields related to small molecules and their protein interactions [11-13].

Visualization and structural inspection of PDB files, as well as docking results, were carried out using PyMOL (version 1.2; http://www.pymol.org), a Python-based molecular graphics tool. Docking simulations were performed using AutoDock 4.2, developed by The Scripps Research Institute (www.scripps.edu). Docking parameters and grid settings were configured through AutoDock Tools (ADT), a user-friendly graphical interface optimized for docking setup and analysis. AutoDock provides a robust computational framework for predicting ligand–protein binding orientations and interaction profiles based on experimentally resolved 3D structures.

Statistical analysis

All experimental data were expressed as the mean ± standard deviation (SD) from at least three independent experiments (n = 3). Differences between multiple groups were analyzed using one-way analysis of variance (ANOVA) followed by Tukey's post hoc test for pairwise comparisons. When only 2 groups were compared, statistical significance was determined using an unpaired Student's t-test. A p-value of less than 0.05 ($p\text{-}value < 0.05$) was considered statistically significant. Graphical data representations (bar charts, line plots, and error bars) were generated in GraphPad Prism and OriginPro 2022a (OriginLab, USA) to ensure clear visualization of intergroup differences. All statistical procedures were conducted in accordance with accepted standards for biomedical data analysis.

Results and discussion

Effect of F-43 on blood pressure dynamics in rats

To assess the hemodynamic profile of compound F-43, systolic blood pressure (SBP) and diastolic blood pressure (DBP) were continuously monitored in conscious rats for three hours after intravenous administration. Two dose levels (25 and 50 mg/kg) were tested to evaluate the dose-dependent influence on vascular tone and cardiac output (**Table 1**).

Table 1 Effect of F-43 compound on systolic (SBP) and diastolic (DBP) blood pressure in rats at doses of 25 and 50 mg/kg over a 3-hour observation period. Data are expressed as mean ± SD (n = 3); no statistically significant differences were observed (*p-value* > 0.05).

	mg/ kg	Baseline		One hour		Two hours		Three hours	
		SBP	DBP	SBP	DBP	SBP	DBP	SBP	DBP
F-43	25	99.0 ± 8.9	66.5 ± 5.8	102.3 ± 9.9	71.3 ± 7.0	87.3 ± 8.5	64.5 ± 6.3	102.3 ± 10	78.5 ± 7.6
	50	126.3 ± 12.4	90.5 ± 8.5	140.8 ± 11.8	115.3 ± 10.5	116.8 ± 11.5	84.0 ± 7.8	108.8 ± 10	67.5 ± 6.2

Prior to drug administration, the baseline values in the 25 mg/kg group were 99.0 ± 8.9 mmHg for SBP and 66.5 ± 5.8 mmHg for DBP, while in the 50 mg/kg group they were slightly higher—126.3 ± 12.4 mmHg and 90.5 ± 8.5 mmHg, respectively. These inter-group variations likely reflect minor individual physiological differences among experimental animals rather than intrinsic treatment effects (**Figure 1**).

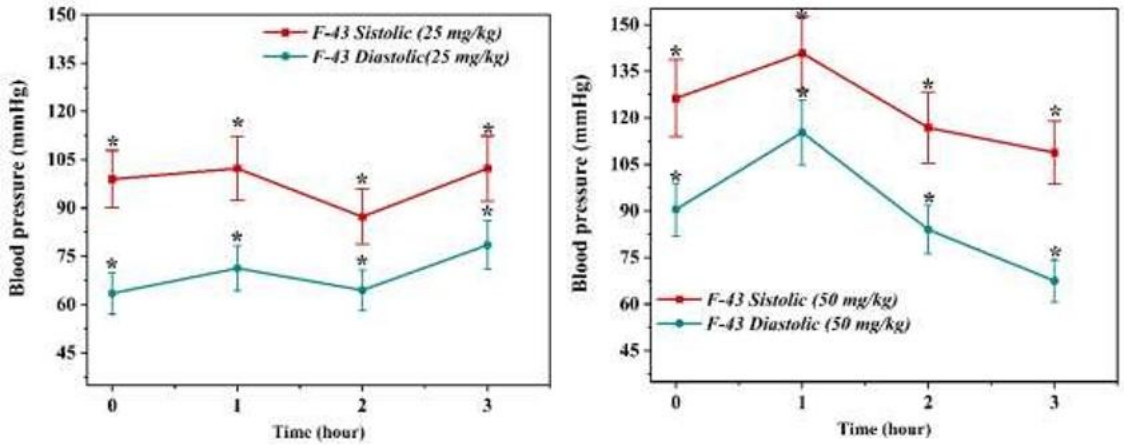

Figure 1 Effect of F-43 at doses of 25 mg/kg (A) and 50 mg/kg (B) on systolic (SBP) and diastolic (DBP) blood pressure. Data are presented as mean ± SD (n = 3). Statistical significance: *p-value* > 0.05.

Following intravenous injection of F-43, both SBP and DBP exhibited dynamic fluctuations over the 3-hour observation period. In the 25 mg/kg group, SBP showed a mild transient increase during the first hour (102.3 ± 9.9 mmHg), followed by a modest reduction to 87.3 ± 8.5 mmHg at the second hour. DBP demonstrated a similar pattern, rising slightly to 71.3 ± 7.0 mmHg at the first hour and decreasing to 64.5 ± 6.3 mmHg at the second hour. By the third hour, both parameters approached baseline levels (SBP = 102.3 ± 10.1 mmHg; DBP = 78.5 ± 7.6 mmHg), indicating a restoration of vascular homeostasis [14,15].

In contrast, the 50 mg/kg dose initially provoked a transient hypertensive response during the first hour (SBP = 140.8 ± 11.8 mmHg; DBP = 115.3 ± 10.5 mmHg), suggesting a short-lived stimulation of vascular contractility or cardiac output. However, this was followed by a progressive normalization: By the second hour SBP and DBP decreased to 116.8 ± 11.5 mmHg and 84.0 ± 7.8 mmHg, respectively, and by the third hour further declined to 108.8 ± 10.2 mmHg and 67.5 ± 6.2 mmHg.

Although these changes did not reach statistical significance (*p-value* > 0.05), the observed trend indicates that F-43 may exert a regulatory effect on vascular tone, initially inducing mild pressor activity followed by a compensatory vasodilatory response. The time-dependent biphasic pattern could reflect the

compound's interaction with both endothelial and smooth muscle signaling systems, possibly involving calcium channel modulation or nitric oxide (NO)-dependent relaxation mechanisms.

Antihypertensive activity of F-43 in the adrenaline-induced hypertension model

To further evaluate the antihypertensive potential of F-43, its effect was tested in an adrenaline-induced hypertension model in rats. This model is characterized by a transient but reproducible elevation of blood pressure following the activation of α- and β-adrenergic receptors, mimicking acute sympathetic overdrive and peripheral vasoconstriction [16,17].

Before the administration of adrenaline, the baseline SBP and DBP in the F-43 group were 98.8 ± 9.6 mmHg and 74.5 ± 6.8 mmHg, respectively. Intravenous injection of adrenaline hydrochloride (10 μg/kg) produced a marked hypertensive response, with SBP rising to 144.8 ± 14.3 mmHg and DBP to 119.0 ± 11.7 mmHg. These changes confirm the successful induction of a hyperadrenergic state leading to systemic vasoconstriction and elevated cardiac workload (**Table 2**).

Table 2 Effect of F-43 (50 mg/kg) on systolic (SBP) and diastolic (DBP) blood pressure in rats with adrenaline- induced hypertension. Blood pressure values were recorded at baseline, after adrenaline administration, and at 1 - 3-hour intervals following F-43 treatment. Data are expressed as mean ± SD (n = 3); *p-value* > 0.05 compared with baseline.

Blood pressure		**Healthy control**	**F-43 (50 mg/kg)**
Baseline	SBP	106,3 ± 10,5	98,8 ± 9,6
	DBP	76,8 ± 7,4	74,5 ± 6,8
Adrenaline 30-minut	SBP	160,5 ± 16,3	144,8 ± 14,3
	DBP	119,5 ± 11,8	119,0 ± 11,7
One hour	SBP	117,8 ± 11,6	133,5 ± 13,5
	DBP	98,8 ± 9,8	94,0 ± 9,3
Two hours	SBP	125,5 ± 12,5	123,5 ± 12,3
	DBP	100,0 ± 10,1	84,3 ± 8,2
Three hours	SBP	119,3 ± 11,8	96,3 ± 8,9
	DBP	94,0 ± 9,2	65,0 ± 6,3

Following this, F-43 was administered intravenously at a dose of 50 mg/kg. Within the first hour, SBP and DBP decreased to 133.5 ± 13.5 mmHg and 94.0 ± 9.3 mmHg, respectively, indicating a partial attenuation of the adrenaline effect (**Figure 2**). During the second hour, a more pronounced decline was observed (SBP = 123.5 ± 12.3 mmHg; DBP = 84.3 ± 8.2 mmHg), and by the third hour, blood pressure values nearly returned to pre-adrenaline levels (SBP = 96.3 ± 8.9 mmHg; DBP = 65.0 ± 6.3 mmHg).

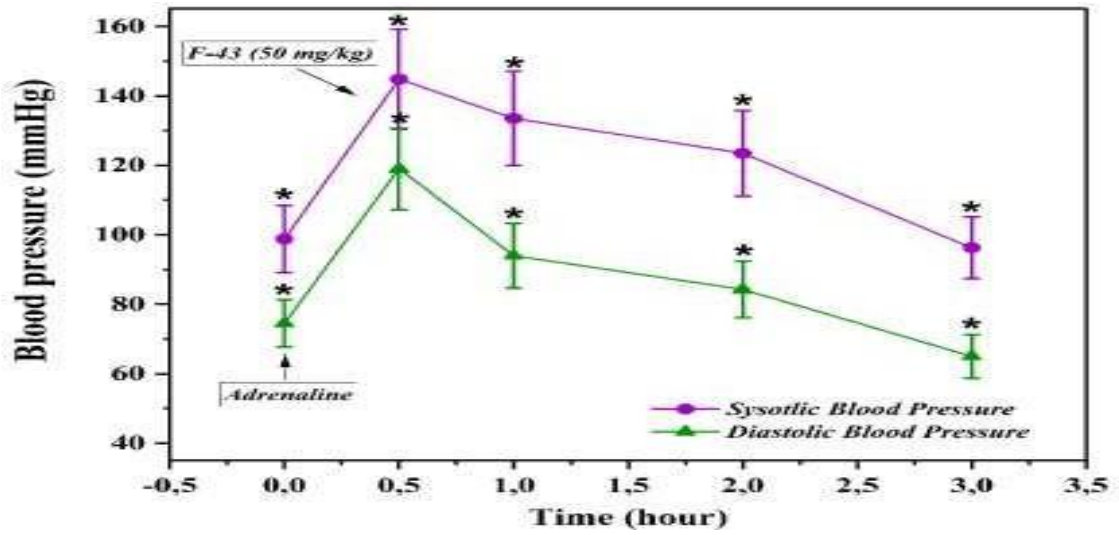

Figure 2 Effect of F-43 (50 mg/kg) on blood pressure in the adrenaline-induced hypertension model. SBP – systolic blood pressure; DBP – diastolic blood pressure. Data are presented as mean ± SD (n = 3); *p-value* > 0.05.

The gradual and sustained normalization of blood pressure over time suggests that F-43 possesses a stable and physiologically compatible antihypertensive action. Unlike many fast-acting vasodilators, which cause abrupt hemodynamic drops, F-43 induced a controlled and progressive restoration of normotension. This feature could be attributed to a balanced modulation of adrenergic signaling, possibly involving antagonistic effects on α_1-adrenergic receptors or the enhancement of endothelial nitric oxide synthase (eNOS) activity [18,19].

Moreover, the pattern of blood pressure recovery implies that F-43 may not act as a simple vasodilator but rather as a homeostatic regulator of vascular reactivity, capable of counteracting adrenergic overstimulation without compromising systemic perfusion. This pharmacodynamic profile makes F-43 a promising candidate for further investigation as a potential antihypertensive or vasoprotective agent [20,21].

In silico analysis of the interaction between F-43 and calcium-handling proteins

To elucidate the potential molecular mechanisms underlying the antihypertensive activity of F-43, its interaction with key calcium-transport proteins was investigated using molecular docking simulations. Four target proteins were selected: The L-type calcium channel (Cav1.2), sarcoplasmic reticulum Ca^{2+}-ATPase (SERCA), ryanodine receptor type-2 (RyR2), and the sodium–calcium exchanger (NCX). Binding affinities and amino acid interactions were analyzed to assess the stability and potential regulatory influence of F-43 on these calcium-handling systems, which play essential roles in vascular smooth muscle contractility and cardiac excitation–contraction coupling [22,23].

Interaction of F-43 with L-type calcium channels

Molecular docking analysis revealed that F-43 exhibited a binding energy of −6.8 kcal/mol with the L-type calcium channel protein (Cav1.2). This value indicates a moderately strong and stable interaction between the ligand and the active binding cavity of the channel. The interaction pattern suggests that F-43 could interfere with calcium influx by modulating channel gating behavior or stabilizing its closed conformation (**Figure 3(A)**). The ligand formed several key non-covalent bonds with amino acid residues crucial for channel activity: Conventional hydrogen and carbon–hydrogen bonds with TYR A:585, TYR A:1035, and ASP A:598; Alkyl and π-alkyl interactions with VAL A:592, ARG A:594, and PRO A:75.

These interactions stabilize the ligand within the transmembrane binding pocket, likely restricting conformational changes necessary for Ca^{2+} conduction. Consequently, F-43 may function as a putative L-type calcium channel modulator, contributing to its observed antihypertensive action.

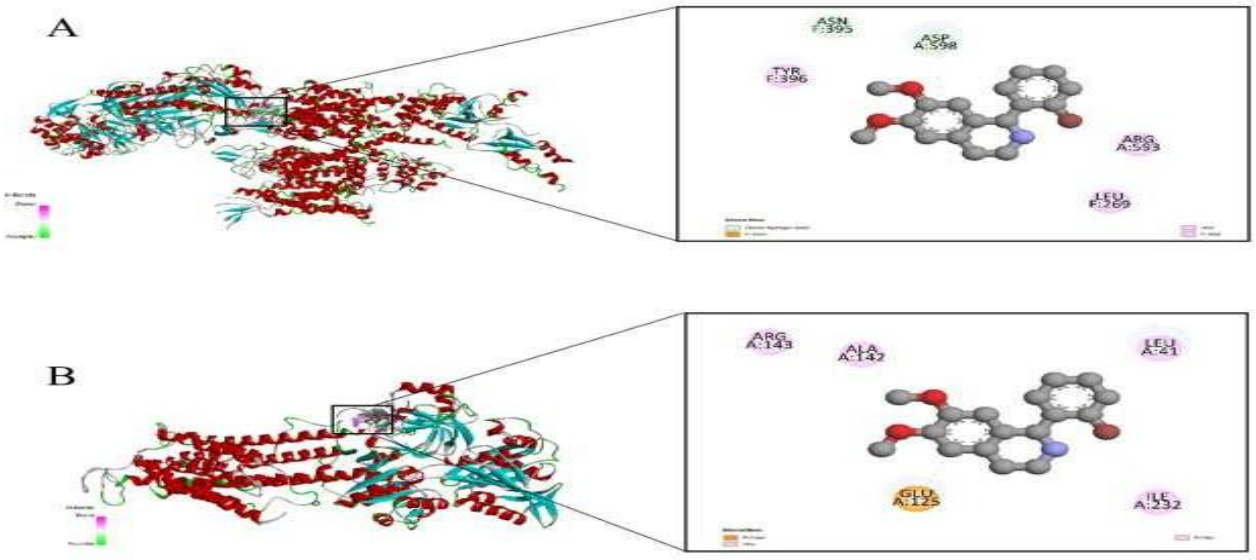

Figure 3 Molecular docking of F-43 with calcium-handling proteins. (A) Binding pose of F-43 within the L-type Ca^{2+} channel (Cav1.2, PDB ID: 6JP5). (B) Interaction of F-43 with the SERCA protein (PDB ID: 6RB2). Key hydrogen-bond and hydrophobic interactions between F-43 and amino-acid residues are highlighted in the magnified 2D interaction maps.

Binding of F-43 to sarcoplasmic reticulum Ca^{2+}-ATPase (SERCA)

Docking simulations demonstrated a binding affinity of −8.7 kcal/mol between F-43 and the SERCA protein, indicating a strong and stable interaction with the enzyme's active domain. Such a low binding energy suggests high ligand– protein affinity and potential inhibitory or modulatory effects on calcium reuptake into the sarcoplasmic reticulum (**Figure 3(B)**).

Detailed analysis revealed multiple stabilizing interactions: π-cation bonding with ARG A:559; Carbon–hydrogen bonding with ASN A:705; π-sulfur interaction with MET A:494;π–π stacking with PHE A:487; Alkyl interactions with LYS A:492.

The engagement of these residues, located near the ATP-binding and translocation domains, implies that F-43 could influence the enzymatic cycling of SERCA and modulate intracellular Ca^{2+} sequestration. This finding supports its role as a potential regulator of calcium homeostasis and vascular relaxation.

Secondary binding mode of F-43 with SERCA

An additional docking run confirmed consistent results, yielding a binding energy of −6.8 kcal/mol. This secondary conformation reinforced the presence of multiple stabilizing interactions within the SERCA cavity: Carbon–hydrogen bonds with GLU A:40, LEU A:41, and PRO A:160; π–anion interaction with GLU A:125; Alkyl and π-alkyl interactions with ILE A:232 and ARG A:143. These results collectively suggest that F-43 can anchor itself near the calcium-binding and phosphorylation domains, potentially reducing the rate of Ca^{2+} reuptake. Functionally, this may prolong cytosolic Ca^{2+} clearance time, contributing to the modulation of vascular smooth muscle contractility and the attenuation of hypertensive responses [24,25].

Interaction of F-43 with ryanodine receptor Type-2 (RyR2)

The docking score for the F-43–RyR2 complex was −6.4 kcal/mol, suggesting a stable and energetically favorable association with the receptor's regulatory site. Given that RyR2 mediates calcium release from the sarcoplasmic reticulum, such an interaction may influence intracellular Ca^{2+} transients and contractile responses (**Figure 4(B)**).

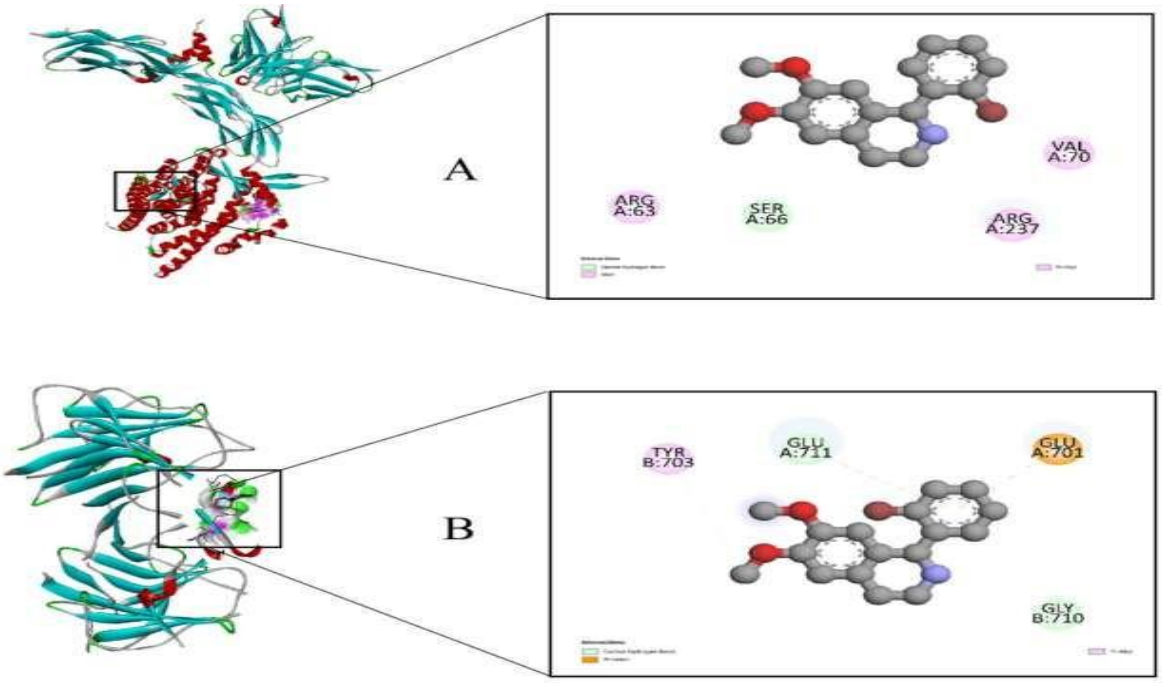

Figure 4 Docking visualization of F-43 with calcium-regulating proteins. (A) Interaction of F-43 with the sodium–calcium exchanger (NCX, PDB ID: 8SGI). (B) Binding of F-43 to the ryanodine receptor type 2 (RyR2, PDB ID: 5C33). Key hydrogen-bond and hydrophobic interactions are highlighted in the 2D maps.

The binding involved the following interactions: Carbon–hydrogen bonds with GLU A:711 and GLU B:710; π–anion bonding with GLU A:701; π-alkyl interactions with TYR B:703. These residues are part of the receptor's cytoplasmic regulatory region, implying that F-43 may stabilize RyR2 in a partially closed or inactive conformation. Thus, the compound may exert a modulatory effect on calcium release, reducing excitatory calcium spikes associated with hypertensive states [26,27].

Interaction of F-43 with the Sodium–Calcium exchanger (NCX)

Molecular docking of F-43 with the NCX transporter yielded a binding energy of −6.8 kcal/mol, indicative of high- affinity and stable complex formation. Since NCX is responsible for Ca^{2+} extrusion in exchange for Na^{+} influx, modulation of this protein can directly affect intracellular Ca^{2+} balance (**Figure 4(A)**). F-43 formed stabilizing contacts with key residues: Carbon–hydrogen bonding with SER A:66; Alkyl and π-alkyl interactions with ARG A:63, ARG A:237, and VAL A:70. The localization of these interactions within the transmembrane domain suggests that F-43 could alter the conformational dynamics of NCX, leading to subtle adjustments in Ca^{2+} efflux and myocardial relaxation. Therefore, F-43 might act as a fine-tuned modulator of NCX activity, complementing its overall antihypertensive profile [28].

Discussion

The present study provides preliminary insight into the hemodynamic and molecular properties of the newly synthesized tetrahydroisoquinoline derivative F-43. Although the *in vivo* experiments were conducted on a small sample size (n = 3), and many measurements did not reach classical statistical significance (*p-value* > 0.05), several physiologically meaningful trends were observed that warrant further investigation.

Hemodynamic response patterns

F-43 produced a biphasic blood pressure response in normotensive rats, characterized by a brief initial increase followed by gradual normalization. This pattern should be interpreted cautiously, as the variability inherent in *in vivo* hemodynamic recordings can yield wide standard deviations. Nevertheless, the tendency toward delayed reduction suggests a possible

modulatory rather than purely hypotensive effect. Similar trend-level responses were observed in the adrenaline-induced hypertension model, where F-43 appeared to attenuate the pressor effect over time. Given the exploratory nature of the study, these observations should be considered hypothesis-generating rather than conclusive.

Putative calcium-regulatory mechanisms

Molecular docking was used solely as a supportive computational approach to explore potential interactions between F-43 and key calcium-handling proteins (Cav1.2, SERCA, RyR2, and NCX). The binding energies observed (−6.4 to −8.7 kcal/mol) are within the range typically associated with ligand–protein association, but they do not confirm functional effects. The docking results therefore provide a theoretical basis for future mechanistic studies rather than evidence of direct modulation.

The interaction patterns suggest that F-43 may have the potential to influence several aspects of calcium homeostasis—such as Ca^{2+} influx through Cav1.2, sequestration by SERCA, release via RyR2, and extrusion through NCX. However, without *in vitro* validation (e.g., patch-clamp recordings, Ca^{2+} imaging, or SERCA activity assays), these possibilities remain speculative. For this reason, mechanistic interpretations have been deliberately softened in the revised manuscript.

Pharmacological implications and limitations

The structural features of F-43, including its methoxy substitutions and tetrahydroisoquinoline scaffold, may support membrane permeability and multi-target binding. However, additional studies—particularly pharmacokinetic, electrophysiological, and chronic dosing assessments—are necessary before firm conclusions can be drawn about its therapeutic potential.

Conclusions

In conclusion, this exploratory study provides preliminary observations on the hemodynamic behavior and predicted molecular interactions of the tetrahydroisoquinoline derivative F-43. Although several blood pressure measurements did not reach statistical significance (*p-value* > 0.05) due to the small sample size and inherent variability of *in vivo* recordings, trend-level responses suggest that F-43 may influence vascular reactivity in both normotensive and adrenaline-induced hypertensive conditions. Molecular docking offered supportive—yet non-confirmatory—insight into possible interactions with calcium-handling proteins such as Cav1.2, SERCA, RyR2, and NCX. These computational findings should be interpreted as hypotheses rather than functional evidence, and they highlight potential mechanistic pathways worthy of further investigation. The study is limited by its small sample size (n = 3), absence of dose–response evaluation, lack of *in vitro* functional validation, and reliance on non-invasive blood pressure measurement. Consequently, the present data do not allow firm conclusions about antihypertensive efficacy but do provide a rationale for continued investigation.

Declaration of Generative AI in Scientific Writing

Only minimal assistance was used from QuillBot for paraphrasing selected sentences. All scientific content, interpretation, and conclusions were developed independently by the authors.

CRediT Author Statement

Ulugbek Gayibov: Conceptualization. **Izzatullo Abdullaev:** Software, Formal Analysis, Docking Simulations, Validation, Writing – Review & Editing. **Ikbolkhon Abdurazakova** and **Makhmudov Lazizbek:** Resources, Data Curation, Sample Preparation, Experimental Support. **Anvar Zaynabiddinov:** Ziyoyiddinov Ziyodullokh: Investigation. **Nodira Abdulladjanova:** Data Collection. **Sherzod Zhurakulov:** synthesis.

References

[1] Sirojiddin, O., Abdullaev, I., Gayibov, U., Torunoğlu, E. İ., & Aytar, E. C. (2026). Cardiovascular effects of Matricaria chamomilla extract: Calcium channel modulation and vasorelaxant activity. Science of Nature, **113(1)**, 14.

[2] Omonturdiev, S., Abdullaev, I., Khasanov, A., Usmonov, P., & Aripov, T. (2026). Molecular mechanisms and experimental protocols in the study of vasorelaxant activity in aortic smooth muscle cells. Trends in Sciences, **23(2)**, 11549.

[3] I Abdullaev, U Gayibov, S Omonturdiev, S Fotima, S Gayibova and T Aripov. Molecular

pathways in cardiovascular disease under hypoxia: Mechanisms, biomarkers, and therapeutic target. *The Journal of Biomedical Research* 2025; **39(3)**, 254-269.

[4] AA Abdullaev, DR Inamjanov, DS Abduazimova, SZ Omonturdiyev, UG Gayibov, SN Gayibova and TF Aripov. *Sílybum Mariánum's* impact on physiological alterations and oxidative stress in diabetic rats. *Biomedical and Pharmacology Journal* 2024; **17(2)**, 1291-1300.

[5] AV Mahmudov, OS Abduraimov, SB Erdonov, UG Gayibov and LY Izotova. Bioecological features of *Nigella sativa* L. in different conditions of Uzbekistan. *Plant Science Today* 2022; **9(2)**, 421-426.

[6] OK Khojimatov, VV Pak and RW Bussmann. *Leonurus turkestanicus V.I. Krecz. & Kuprian., Leonurus panzerioides Popov - LAMIACEAE*. *In*: OK Khojimatov, Y Gafforov and RW Bussmann. (Eds.). Ethnobiology of uzbekistan. Ethnobiology, Springer, Cham, 2023.

[7] AQQ Azimova, AX Islomov, SA Maulyanov, DG Abdugafurova, LU Mahmudov, IZ Abdullaev, AS Ishmuratova, SQ Siddikova and IR Askarov. Determination of vitamins and pharmacological properties of *Vitis vinifera* L. plant fruit part (mixed varieties) syrup-honey. *Biomedical and Pharmacology Journal* 2024; **17(4)**, 2779-2786.

[8] Abdurazakova, I., Zaynabiddinov, A., Abdullaev, I., Xolmirzayeva, M., & Zhurakulov, S. (2025). Pharmacological evaluation of F45 on the cardiovascular system using in vitro, in vivo models and molecular docking. Trends in Sciences, **22(12)**, 10924.

[9] O Gaibullayeva, A Islomov, D Abdugafurova, B Elmurodov, B Mirsalixov, L Mahmudov, I Adullaev, K Baratov, S Omonturdiev and S Sa'Dullayeva. *Inula helenium* L. root extract in sunflower oil: Determination of its content of water-soluble vitamins and immunity-promoting effect. *Biomedical and Pharmacology Journal* 2024; **17(4)**, 2729-2737.

[10] A Abdullaev, I Abdullaev, A Bogbekov, U Gayibov, S Omonturdiev, S Gayibova, M Turahodjayev, K Ruziboev and T Aripov. Antioxidant potential of *Rhodiola heterodonta* extract: Activation of Nrf2 pathway via integrative *in vivo* and *in silico* studies. *Trends in Sciences* 2025; **22(5)**, 9521.

[11] OS Zoirovich, AIZ Ugli, ID Raxmatillayevich, ML Umarjonovich, ZM Ravshanovna and G Sabina. The effect of Ájuga Turkestánica on the rat aortic smooth muscle ion channels. *Biomedical and Pharmacology Journal* 2024; **17(2)**, 1213-1222.

[12] D Inomjonov, I Abdullaev, S Omonturdiev, A Abdullaev, L Maxmudov, M Zaripova, M Abdullayeva, D Abduazimova, S Menglieva, S Gayibova, M Sadbarxon, U Gayibov and T Aripov. *In vitro* and *In vivo* studies of *Crategus* and *Inula helenium* extracts: Their effects on rat blood pressure. *Trends in Sciences* 2025; **22(3)**, 9158.

[13] S Sodiqova, S Kadirova, A Zaynabiddinov, I Abdullaev, L Makhmudov, U Gayibov, M Yuldasheva, M Xolmirzayeva, R Rakhimov, A Mutalibov and H Karimjonov. Channelopathy activity of A- 41(Propyl Ester of Gallic Acid): Experimental and computational study of antihypertensive activity. *Trends in Sciences* 2025; **22(9)**, 10496.

[14] R Sayidaliyeva, S Kadirova, A Zaynabiddinov, I Abdullaev, L Makhmudov, U Gayibov, M Yuldasheva, M Kholmirzayeva, R Rakhimov, A Mutalibov and H Karimjonov. A-51 as a natural calcium channel blocker: An integrative study targeting hypertension. *Trends in Sciences* 2025; **22(11)**, 10760.

[15] A Khasanov, I Abdullaev, S Kadirova, M Mamajanov, A Zaynabiddinov, S Omonturdiev, L Makhmudov, D Inomjonov, U Gayibov, R Esanov and A Matchanov. N-2 polyphenol targets vascular calcium channels to exert antihypertensive effects: *In vitro* and *in vivo* evaluation. *Trends in Sciences* 2025; **22(12)**, 10782.

[16] NR Djuraeva, KS Rakhmonov, NR Barakayev, TI Atamuratova, ME Mukhamedova and KM Muzafarova. Plant-fat mixtures as potential raw material for bakery production. *Plant Cell Biotechnology and Molecular Biology* 2020; **21(45-46)**, 29-42.

[17] M Zaripova, I Abdullaev, A Bogbekov, U Gayibov, S Omonturdiev, R Makhmudov, N

Ergashev, G Jabbarova, S Gayibova and T Aripov. *In vitro* and *in silico* studies of gnaphalium U. Extract: Inhibition of α-amylase and α-glucosidase as a potential strategy for metabolic syndrome regulation. *Trends in Sciences*, 2025; **22(8)**, 10098.

[18] UG Gayibov, SN Gayibova, DS Abduazimova, RN Rakhimov, HS Ruziboev, MA Xolmirzayeva, AE Zaynabiddinov and TF Aripov. Antioxidant and cardioprotective properties of polyphenolic plant extract of *Rhus glabra* L. *Plant Science Today* 2024; **11(3)**, 2348-1900.

[19] TF Aripov and UG Gayibov. Antiradical and antioxidant activity of the preparation "Rutan" from *Rhus coriaria* L. *Journal of Theoretical and Clinical Medicine* 2023; **4**, 164-170.

[20] MR Zaripova, SN Gayibova, RR Makhmudov, AA Mamadrahimov, NL Vypova, UG Gayibov, SM Miralimova and TF Aripov. Characterization of *Rhodiola heterodonta* (Crassulaceae): Phytocomposition, antioxidant and antihyperglycemic activities. *Preventitive Nutrition Food Science* 2024; **29(2)**, 135-145.

[21] AV Mahmudov, OS Abduraimov, SB Erdonov, AL Allamurotov, OT Mamatkasimov, UG Gayibov and LY Izotova. Seed productivity of *Linum usitatissimum* L. in different ecological conditions of Uzbekistan. *Plant Science Today* 2022; **9(4)**, 1090-1101.

[22] M Mamajanov, I Abdullaev, G Sotimov, S Mavlanova, Q Niyozov, M Mirzaolimov, A Najimov, E Mirzaolimov, M Raximberganov and U Abdullayev. Mitochondrial and pharmacokinetic insightsinto 3,5,7,2′,6′-pentahydroxyflavanone. *Trends in Sciences* 2025; **22(12)**, 10984.

[23] TF Aripov, UG Gayibov, SN Gaibova, YI Oshchepkova and ShI Salikhov. *In vitro* antioxidant and antiradical activity of the total polyphenols (substances of the antiviral drug Rutan) of the leaves of tannic sumach Rhus coriaria L. *Low-Molecular Compounds* 2024; **4**, 138-147.

[24] UG Gayibov, EJ Komilov, RN Rakhimov, NA Ergashev, NG Abdullajanova, MI Asrorov and TF Aripov. Influence of new polyphenol compound from Euphorbia plant on mitochondrial function. *Journal of Microbiology Biotechnology and Food Science* 2019; **8(4)**, 1021-1025.

[25] Y Umidakhon, B Erkin, G Ulugbek, N Bahadir and A Karim. Correction of the mitochondrial NADH oxidase activity, peroxidation and phospholipid metabolism by haplogenin-7-glucoside in hypoxia and ischemia. *Trends in Sciences* 2022; **19(21)**, 6260.

[26] MK Pozilov, U Gayibov, MI Asrarov, NG Abdulladjanova, HS Ruziboev and TF Aripov. Physiological alterations of mitochondria under diabetes condition and its correction by polyphenol gossitan. *Journal of Microbiology Biotechnology and Food Science* 2022; **12(2)**, e2224.

[27] AG Vakhobjonovna, KE Jurayevich, AIZ Ogli, EN Azamovich, MR Rasuljonovich and AM Islomovich. Tannins as modulators in the prevention of mitochondrial dysfunction. *Trends in Sciences* 2025; **22(8)**, 10436.

[28] Z Shakiryanova, R Khegay, U Gayibov, A Saparbekova, Z Konarbayeva, A Latif and O Smirnova. Isolation and study of a bioactive extract enriched with anthocyanin from red grape pomace (Cabernet Sauvignon). *Agronomy Research* 2023; **21(3)**, 1293-1303.

[29] U Gayibov, SN Gayibova, KP Ma'Murjon, FS Tuxtaeva, UR Yusupova, GMK Djabbarova, ZA Mamatova, NA Ergashev and TF Aripov. Influence of quercetin and dihydroquercetin on some functional parameters of rat liver mitochondria. *Journal of Microbiology, Biotechnology and Food Sciences* 2021; **11(1)**, 2924.